



UNIVERSITÀ
DEGLI STUDI
FIRENZE

FLORE

Repository istituzionale dell'Università degli Studi di Firenze

Modeling Litz-wire winding losses in high-frequency power inductorsPESC Record. 27th Annual IEEE Power Electronics

Questa è la Versione finale referata (Post print/Accepted manuscript) della seguente pubblicazione:

Original Citation:

Modeling Litz-wire winding losses in high-frequency power inductorsPESC Record. 27th Annual IEEE Power Electronics Specialists Conference / M. Bartoli;N. Noferi;A. Reatti;M.K. Kazimierczuk. - ELETTRONICO. - 2:(1996), pp. 1690-1696. (Power Electronics Specialists Conference, 1996. PESC '96 Record., 27th Annual IEEE) [10.1109/PESC.1996.548808].

Availability:

The webpage <https://hdl.handle.net/2158/645184> of the repository was last updated on

Published version:

DOI: 10.1109/PESC.1996.548808

Terms of use:

Open Access

La pubblicazione è resa disponibile sotto le norme e i termini della licenza di deposito, secondo quanto stabilito dalla Policy per l'accesso aperto dell'Università degli Studi di Firenze (<https://www.sba.unifi.it/upload/policy-oa-2016-1.pdf>)

Publisher copyright claim:

La data sopra indicata si riferisce all'ultimo aggiornamento della scheda del Repository FloRe - The above-mentioned date refers to the last update of the record in the Institutional Repository FloRe

(Article begins on next page)

Modeling Litz-Wire Winding Losses in High-Frequency Power Inductors

Massimo Bartoli, Nicola Noferi, Alberto Reatti, Member, IEEE
University of Florence, Department of Electronic Engineering,
Via S. Marta 3, 50139, Florence, ITALY
Fax +39-55-494569. E-mail: circuiti@speedynet.it

Marian K. Kazimierczuk, Senior Member, IEEE
Wright State University, Department of Electrical Engineering,
45435, Dayton, OH.
Fax 513-873-5009. E-mail: mkazim@valhalla.cs.wright.edu

Abstract—The parasitic effects in stranded, twisted, and *Litz* wire windings operating at high frequencies are studied. The skin and proximity effects that cause the winding parasitic resistance of an inductor to increase with the operating frequency are considered. An expression for the ac resistance as a function of the operating frequency is given. The measured and calculated values of the inductor ac resistance and quality factor are plotted versus frequency and compared. The theoretical results were in good agreement with those experimentally measured.

I. INTRODUCTION

The overall efficiency of power circuits such as power converters and power amplifiers highly depends on the efficiency of inductors used in assembling the circuit. Therefore, the control of power losses in magnetic components is important for increasing the efficiency of the overall circuit. One of the main problems related to the design of power inductors is the calculation of the winding ac resistance R_{ac} . Many efforts [1]–[6] have been made to derive expressions allowing for an accurate representation of frequency behavior of R_{ac} .

Stranded, twisted, and *Litz* wires are commonly thought to result in lower ac resistances than solid wires. This is because the current through a solid wire concentrates in the external part of the conductor at high operating frequencies. If a multistrand

conductor is used, the overall cross-sectional area is spread among several conductors with a small diameter. For this reason, stranded, twisted, and *Litz* wire results in a more uniform current distribution across the wire section. Moreover, *Litz* wires are assembled so that each single strand, in the longitudinal development of the wire, occupies all the positions in the wire cross section. Therefore, not only the skin effect but also proximity effect is drastically reduced. However, the following limitations occur when using *Litz* wires:

- 1) The utilization of the winding space inside a bobbin width is reduced with respect to a solid wire.
- 2) The dc resistance of a *Litz* wire is larger than that of a solid wire with the same length and equivalent cross-sectional area because each strand path is longer than the average wire length.

Consequently, a *Litz* wire results in a lower ac resistance than a solid wire only if the multistrand wire windings are operated in an appropriate frequency range. This range can be predicted only if an expression for the winding ac resistance of a *Litz* wire as a function of frequency is available.

The purposes of this paper are (1) to derive an accurate analytical expression for *Litz* wire winding ac resistance suitable for designing of low-loss high-frequency power inductors, (2) to compare the ac resistances of *Litz* and solid wires, and (3) to ver-

ify the theoretical predictions with experimental results.

The significance of the paper is that the derived expression for ac resistances allows for an accurate prediction of the frequency behavior of an inductor *Litz*-wire windings. Both the expression for R_{ac} and the inductor model can be used to design inductors for high frequency operation with reduced winding losses.

II. LITZ WIRE AC RESISTANCE

In [1], the analytical expression for the ac resistance of a solid wire winding has been derived under the following assumptions:

- 1) The one-dimensional approach proposed in [2] and [3] has been followed.
- 2) A high magnetic permeability has been assumed for the core material. Moreover, it was assumed that the winding layer wires fill the entire breadth of the bobbin. Under these assumptions, the magnetic component behavior is close to that of an ideally infinite long solenoid winding.
- 3) The curvature of the windings is neglected in calculating the magnetic field distribution across the winding layers.
- 4) The orthogonality principle [4],[5] has been applied.

The main advantage of this approach is that it allows for the calculation of the overall ac resistance of a solid round wire as the sum of an ac resistance due to the skin effect and an ac resistance due to the proximity effect. The ac resistance of multiwire conductors, e.g., *Litz* wires, is due to four different parasitic effects:

- 1) skin effect in each single strand of the bundle.
- 2) skin effect on the overall bundle that causes the absence of current in the internal strands;
- 3) proximity effect between the single strands;
- 4) proximity effect between the bundles of the different turns.

The proximity and skin effects can be assumed to be independent from each other, that is, the orthogonality principle can be applied to multiwire windings along with the other assumptions used for the

solid wire windings. The twisted wires have the advantage of lower proximity losses than the stranded ones. Actually, the internal strands are wound together, so that each single strand has an helicoidal movement around the center of the bundle, with a constant distance from the center itself. Since z is the longitudinal axis along the direction of the bundle and λ is the twisting pitch, the instantaneous phase of the helix with respect to the center of the bundle $J(z)$ is given by

$$\vartheta(z) = 2\pi \frac{z}{\lambda}. \quad (1)$$

In the expression for the current density inside the twisted wire, a multiplying factor $\sin J(z)$ is contained. Averaging this effect over one wavelength λ , one obtains:

$$\frac{1}{\lambda} \int_0^\lambda \sin^2 \vartheta(z) dz = \frac{1}{2}. \quad (2)$$

Twisting allows a 50% reduction of the proximity losses. However, there are no evident advantages of reducing the skin effect. Improvements in this direction can be achieved by the use of *Litz* wire.

Litz wire is a bundle of strand conductors, where the strands are twisted with others so that all the strands alternatively occupy all the positions of the wire cross section. With respect to a the twisted wires, in the *Litz* wires the strand distance to the center of the bundle is not fixed. This allows the current to flow also in the internal strands even at higher frequencies and a more uniform current distribution is achieved. In this way, an averaging of the overall skin effect is obtained and also at high frequencies, the current density due to the mere skin effect is almost the same in all the strands. Previous considerations allow us to deduce an analytical expression for the ac resistance of a *Litz* wire winding in the following way.

Taking the one-dimensional approach [2], [3], and using the orthogonality principle, [4], [5], an analytical expression for the ac resistance of a coil winding has been derived in [1]. For a solid round wire winding composed of N_l layers, the procedure given in [1] yields:

$$R_w = R_{dc} \frac{\gamma}{2} \left\{ \frac{\text{ber} \gamma \text{bei}' \gamma - \text{bei} \gamma \text{ber}' \gamma}{\text{ber}'^2 \gamma + \text{bei}'^2 \gamma} - 2\pi \eta^2 \left(\frac{4(N_l^2 - 1)}{3} + 1 \right) \right\} \quad (3)$$

$$\frac{\text{ber}_2\gamma\text{ber}'\gamma - \text{bei}_2\gamma\text{bei}'\gamma}{\text{ber}^2\gamma + \text{bei}^2\gamma} \Big\}$$

where

$$\gamma = \frac{d}{\delta\sqrt{2}} \quad (4)$$

$$\eta = \text{porosity factor} = \frac{d}{t} \sqrt{\frac{\pi}{4}} \quad (5)$$

and

$$R_{dc} = r_L N l_T = \frac{4\rho}{\pi d^2} N l_T \quad (6)$$

is the dc winding resistance, $\delta = \sqrt{\pi f \mu_o \mu_r \sigma}$ is the skin depth, μ_r is the relative magnetic permeability of the conductor material ($\mu_r = 1$ for a copper conductor), $\mu_o = 4\pi 10^{-10}$ H / mm, d is the solid round conductor diameter in mm, t is the distance between the centers of two adjacent conductors in mm, N is the number of turns of the winding, l_T (mm) is the average length of one turn of the winding, and ρ is the conductor resistivity at a given operating temperature ($\rho = 17.24 \times 10^{-6}$ Ω mm for a copper conductor at an operating temperature of 20 °C). Wire data sheets usually give values of r_L at 20 °C and 100 °C; the latter is typically 1.33 times the former.

This approach can be applied also to *Litz* wire and it allows for calculating the skin effect losses separately from the proximity ones. In Fig. 1, the cross section of a *Litz* wire conductor subjected to an external magnetic field H_e is shown.

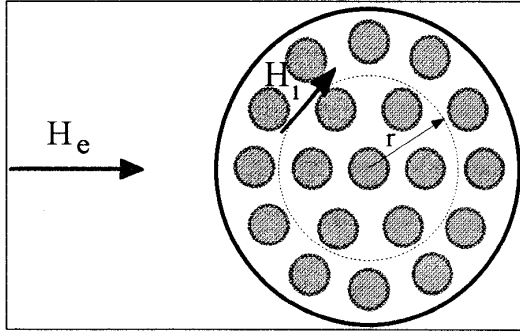


Fig. 1. Cross section of a *Litz* wire.

The analytical expression for the ac resistance of the *Litz* wire winding has been derived under the following assumptions:

- 1) The one-dimensional approach proposed in [2] and [3] has been followed

- 2) The expression derived for the ac resistance is in the rectangular coordinates and is deduced approximating a winding layer to a foil conductor with the magnetic field assumed to be parallel to the conductor surface.

- 3) Assumptions 1) and 2) are guaranteed if the core material has a high magnetic permeability, and the winding layer wires fill the entire breadth of the bobbin. Under these assumptions, the magnetic component behavior is close to that of an ideally infinite long solenoid windings.

- 4) The curvature of the windings is neglected when calculating the magnetic field distribution across the layers.

These assumptions are the same as those utilized in [1] to deduce expression (3):

If only the skin effect is considered and a current I_m/n_s , where n_s is the number of strands, is assumed to flow through each strand, the power losses of the m -th layer of the winding are given by

$$P_{s \text{ strand } m} = \frac{1}{2} R_{s \text{ strand } m} \left(\frac{I_m}{n_s} \right)^2$$

where $R_{s \text{ strand } m}$ is given by [1]

$$R_{s \text{ strand } m} = R_{dc \text{ strand } m} \frac{\gamma_s}{2} \frac{\text{ber}\gamma_s \text{bei}\gamma_s - \text{bei}\gamma_s \text{ber}\gamma_s}{\text{ber}^2\gamma_s + \text{bei}^2\gamma_s} \quad (7)$$

where $\gamma_s = d_s/\delta\sqrt{2}$ and $d_s = 2r_s$ is the single strand conductor diameter in mm, and $R_{dc \text{ strand } m}$ is the internal strand dc resistance.

The skin effect losses may be approximated by the sum of the effects in the n_s *Litz* wire internal strands. Moreover, thanks to the *Litz* wire geometry the overall skin effect in the bundle can be neglected. As a consequence, power losses in the m -th layer of the winding can be calculated as

$$\begin{aligned} P_{s \text{ } m} &= n_s \cdot \frac{1}{2} R_{s \text{ strand } m} \left(\frac{I_m}{n_s} \right)^2 \\ &= \frac{1}{2} \frac{R_{s \text{ strand } m}}{n_s} I_m^2. \end{aligned} \quad (8)$$

Lets now evaluate the contributions of the two proximity effect components (internal and external) to the power losses. It has been demonstrated in [5]

that the overall proximity losses can be calculated as the sum of the contributions due to the internally generated magnetic field (H_i) and to the external one (H_e):

$$P_{p\ m} = P_{p\ m\ int} + P_{p\ m\ ext}. \quad (9)$$

Under the assumption that all the strands in the bundle behave in the same way with respect to the external field, $P_{p\ m\ ext}$ is given by [1]:

$$\begin{aligned} P_{p\ m\ ext} &= n_s \eta_1^2 K_{2\ strand} H_e^2 \\ &= \frac{1}{2} R_{p\ m\ ext} I_m^2 \end{aligned} \quad (10)$$

where

$$K_{2\ strand} = -\frac{2\pi\gamma_s}{\sigma} \frac{ber_2\gamma_s ber\gamma_s + bei_2\gamma_s bei\gamma_s}{ber^2\gamma_s + bei^2\gamma_s} \quad (11)$$

$$\eta_1 = \text{external porosity factor} = \frac{d_s}{t_o} \sqrt{\frac{\pi}{4}} \quad (12)$$

where t_o is the distance between the centers of two adjacent *Litz* wire conductors.

A good approximation of the overall internal proximity losses is given by [1], [5]:

$$P_{p\ m\ int} = \frac{n_s \eta_2^2 K_{2\ strand} I_m^2}{8\pi^2 r_o^2} \quad (13)$$

where

$$\eta_2 = \text{internal porosity factor} = \frac{d_s}{t_s} \sqrt{\frac{\pi}{4}} \quad (14)$$

r_o is the *Litz* wire radius excluding the insulating layer and t_s is the distance between the centers of two adjacent strands, taking into account the effective turn-to-turn, layer-to-layer, and strand-to-strand distances and the non-uniformity of the magnetic field.

In [1], the importance of the introduction in (3) of the porosity factor, η^2 , has been underlined. Actually, it takes into account the effective turn-to-turn and layer-to-layer distances and the absence of uniformity of the magnetic field. For these same reasons, coefficients η_1 and η_2 have been introduced also in (10) and (13), respectively. The introduction

of two different factors is necessary in the analysis of *Litz* wires because of the geometrically different operating influences of the external (H_e) and internal (H_i) magnetic field on the single strand of the bundle. The two proximity components of the ac resistance, for the m -th layer of a *Litz* wire winding, are then given by

$$R_{p\ m\ ext} = R_{dc\ strand\ m} \frac{\gamma_s}{2} \left[-2\pi n_s \eta_1^2 \frac{ber_2\gamma_s ber'\gamma_s - bei_2\gamma_s bei'\gamma_s}{ber^2\gamma_s + bei^2\gamma_s} \right] \quad (15)$$

and

$$R_{p\ m\ int} = R_{dc\ strand\ m} \frac{\gamma_s}{2} \left[-2\pi \eta_2^2 \frac{p}{2\pi} \frac{ber_2\gamma_s ber'\gamma_s - bei_2\gamma_s bei'\gamma_s}{ber^2\gamma_s + bei^2\gamma_s} \right] \quad (16)$$

where the packing factor of a *Litz* wire is defined as

$$p = \frac{N\pi r_s^2}{\pi r_o^2} \quad (17)$$

and $d_o = 2r_o$ is the *Litz* wire diameter excluding the insulating layer.

From (7), (15) and (16) and applying the orthogonality principle as done in [1] to obtain (3), the overall ac resistance for the m -th layer is given by

$$\begin{aligned} R_{w-m} &= R_{dc-m} \frac{\gamma_s}{2} \left\{ \frac{1}{n_s} \frac{ber\gamma_s bei'\gamma_s - bei\gamma_s ber'\gamma_s}{ber'^2\gamma_s + bei'^2\gamma_s} \right. \\ &\quad - 2\pi (2m-1)^2 n_s \left(\eta_1^2 + \eta_2^2 \frac{p}{2\pi n_s} \right) \\ &\quad \left. \frac{ber_2\gamma_s ber'\gamma_s - bei_2\gamma_s bei'\gamma_s}{ber^2\gamma_s + bei^2\gamma_s} \right\}. \end{aligned} \quad (18)$$

As a consequence, if an N_l -layer *Litz* wire winding is considered, where all layers have the same number of turns and then the same $R_{dc\ strand\ m}$, its overall ac resistance can be calculated as follow:

$$\begin{aligned} R_w &= R_{dc} \frac{\gamma_s}{2} \left\{ \frac{1}{n_s} \frac{ber\gamma_s bei'\gamma_s - bei\gamma_s ber'\gamma_s}{ber'^2\gamma_s + bei'^2\gamma_s} \right. \\ &\quad - 2\pi \left[\frac{4(N_l^2 - 1)}{3} + 1 \right] \\ &\quad n_s \left(\eta_1^2 + \eta_2^2 \frac{p}{2\pi n_s} \right) \\ &\quad \left. \frac{ber_2\gamma_s ber'\gamma_s - bei_2\gamma_s bei'\gamma_s}{ber^2\gamma_s + bei^2\gamma_s} \right\} \end{aligned} \quad (19)$$

where

$$R_{dc} = \frac{4\rho}{n_s \pi d_s^2} N l_T \quad (20)$$

is the *Litz* wire dc resistance, N is the number of turns of the winding, l_T (mm) is the average length of one turn of the winding.

The expression for the ac resistance given in (19) provides an accurate prediction of the *Litz* wire ac resistance over a wide frequency range. Moreover, it also allows for choosing the *Litz* wire with the lowest resistance for any given application. The theoretical results are in good agreement with the experimental tests. The results of this paper can be effectively used in the design of high quality factor, low-loss, high-frequency power inductors.

III. COMPARISON OF LITZ AND SOLID ROUND WIRE RESISTANCES

Two different windings with a nearly equal dc resistance are considered as follows:

- 1) solid round wire AWG#28, with $d = 0.32$ mm, transversal conducting area $A = 0.081$ mm², and $d_{ext} = 0.37$ mm;
- 2) *Litz* wire 20×0.08, with a number of strands $n_s = 20$, conducting diameter $d_s = 0.08$ mm, a total transversal conducting area $A = 0.1005$ mm², and $d_{ext} = 0.554$ mm.

Both wires have been wound on the same E-25 Micrometals core with a number of turns $N = 114$ in order to provide the same inductance. The solid round wire results in a 3-layer winding and *Litz* in more than a 4-layer winding.

In Fig. 2, two winding ac resistances calculated from (19) are plotted as functions of the inductor operating frequency. These plots show that the ac resistance of a *Litz* wire winding is lower than that of a solid round wire in a frequency range from 20 kHz to 800 kHz. Above this frequency, the *Litz* wire resistance becomes much higher than the solid wire resistance. This demonstrates that *Litz* wire provides lower losses only in a limited frequency range. Since at low frequencies the dc resistances of the two wires are nearly the same, the solid round wire is preferred because of its better utilization of the winding width.

In Fig. 3, the resistances of a solid round wire, and *Litz* wire windings with a different number of strands are compared. The wire overall cross-sectional areas were chosen to result in the same dc resistance. The plots of Fig. 3 lead to the following conclusions:

- 1) The *Litz* and solid wire conductors have the same resistance up to $f = 10 \div 15$ kHz, depending on the number of strands.
- 2) The ac resistances of *Litz* wires are lower than the solid wire resistances in a frequency range depending on the number of strands as follows

$15 \div 800$ kHz	for a 10 strand <i>Litz</i> wire;
15 kHz \div 1 MHz	for a 20 strand <i>Litz</i> wire;
15 kHz \div 1.7 MHz	for a 60 strand <i>Litz</i> wire.
- 3) For frequencies higher than those shown above the *Litz* wire ac resistances are higher than the solid wire resistances.

Therefore, if the number of strands of the *Litz* wire is increased, its ac resistance is lower and is lower than that of a solid round wire over a wider frequency range. The limitation of a high strand number *Litz* wire is that it has a large winding displacement.

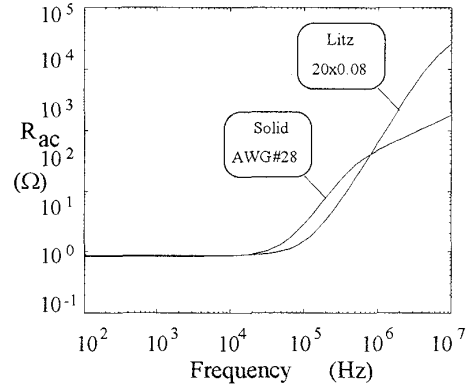


Fig. 2. Resistances R_{ac} of a solid and *Litz* wire versus frequency.

IV. EXPERIMENTAL RESULTS

To verify the accuracy of expression (19), the lumped-parameter equivalent circuit of inductors

shown in Fig. 4 was used. In Fig. 4(a), L is the nominal inductance, R_{ac} is the winding resistance, R_c is the magnetic core resistance, and C is the inductor self-capacitance. Both resistances are frequency dependent and, if the core resistance R_c is much lower than the winding ac resistance R_{ac} , the inductor model simplifies to the form depicted in Fig. 4(b). Most LCR meters measure an equivalent series reactance X_s and an equivalent series resistance R_s of two-terminal devices as shown in Fig. 4(c). The impedance of the equivalent circuit of Fig. 4(c) is

$$Z_s = \frac{R_{ac} + j\omega L \left(1 - \omega^2 LC - \frac{CR_{ac}^2}{L}\right)}{(1 - \omega^2 LC)^2 + \omega^2 C^2 R_{ac}^2} = R_s + jX_s. \quad (21)$$

For frequencies f much lower than the first self-resonant frequency f_r , the equivalent series reactance X_s has an inductive character and can be expressed as $X_s = \omega L_s$. Hence, the equivalent series inductance is $L_s = X_s/\omega$ as shown in Fig. 4(d). The inductor quality factor at a given frequency is

$$Q = \frac{|X_s|}{R_s} = \frac{\left| \omega L \left(1 - \omega^2 LC - \frac{CR_{ac}^2}{L}\right) \right|}{R_{ac}}. \quad (22)$$

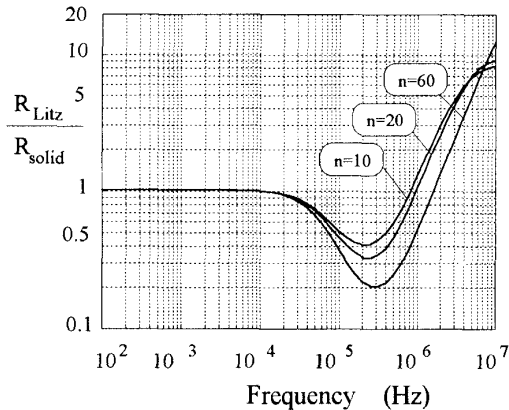


Fig. 3. Resistances R_{ac} of 10 strands Litz wire, 20 strands Litz wire, and 60 strands Litz wire normalized with respect to a solid round wire resistance.

To verify the accuracy of expression (19), tests were performed using an HP4192A "LF Impedance Analyzer" equipped with an HP16047A test fixture to achieve a higher accuracy in minimizing residual parameters and contact resistances. The inductor with negligible core losses was built using low-

permeability core materials. Tests have been performed on an inductor assembled with 114 turns in 4-layers of Litz 20×0.08 wire wound on a Micrometals E25 material mix #52 with $\mu_r=75$ core with a gapped central leg of 9 mm and an effective magnetic permeability $\mu_e=6$. An inductance of $L = 168 \mu\text{H}$ and a resonance frequency $f_r = 2.620 \text{ MHz}$ were measured.

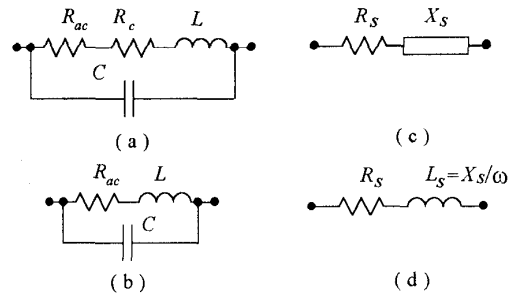


Fig. 4. Equivalent circuit of inductors. (a) Lumped parameter equivalent circuit. (b) Simplified equivalent circuit for $R_c \ll R_{ac}$. (c) Series equivalent circuit. (d) Equivalent circuit assumed by many LCR meters.

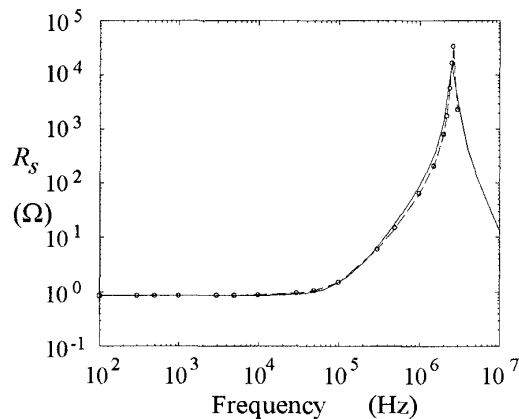


Fig. 5. Equivalent series resistance R_s of the experimentally tested inductor. — calculated; o-o- measured.

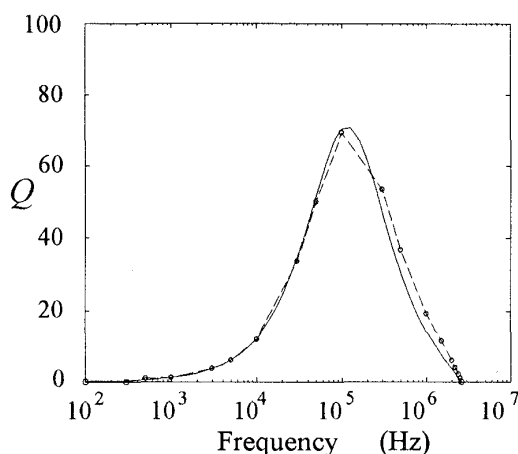


Fig. 6. Quality factor Q of the experimentally tested inductor. — calculated; o-o- measured.

Fig. 6 shows the plots of the theoretical and measured equivalent series resistances of the inductor modelled as in [6]-[8]. Note that R_s is approximately one hundred times R_{dc} at 1 MHz and R_s increases at higher frequencies. The plots of the inductor quality factor Q is shown in Fig. 6. Theoretical and experimental results were in good agreement.

V. CONCLUSIONS

An expression for the ac resistance of inductor winding wound by using *Litz* wire has been derived. The accuracy of this expression has been verified by comparing theoretical results with experimental results derived from testing an iron-powder core inductor. A relatively large air gap was introduced to minimize the core losses. The theoretical results were in agreement with measured results.

The expression for the *Litz* wire winding ac resistance was used to compare the frequency behavior of *Litz* wire and solid wire windings. This comparison has shown that the resistances of the windings remains nearly the same up to about 15 kHz. For frequencies higher than 12-18 kHz, the ac resistance of *Litz* wire winding is much lower than that of solid wire windings. At frequencies higher than some hundreds of kilohertz, the solid wire results in a lower ac resistance than the *Litz* wire.

The expression for the ac resistance for *Litz* wire winding shown in this work, along with the expression for the solid wire winding shown in other papers

by the same authors, can be used to design power inductor with reduced power losses. Therefore, this paper represents an useful tool for designing high-efficiency power converter.

The extension of the presented results to inductor winding operated at non sinusoidal current such as in inductors used in PWM DC-DC converters is highly recommended.

REFERENCES

- [1] M. Bartoli, N. Noferi, A. Reatti, and M. K. Kazimierczuk, "Modelling winding losses in high-frequency power inductors," *World Scientific Journal of Circuits, Systems and Computers*, Special Issue on Power Electronics, Part II, vol. 5, No. 4, pp. 607-626, Dec. 1996.
- [2] E. Bennet and S. C. Larson, "Effective resistance of alternating currents of multilayer windings," *Transactions of American Institute of Electrical Engineering*, vol. 59, pp. 1010-1017, 1940.
- [3] M. P. Perry, "Multiple layer series connected winding design for minimum losses," *IEEE Trans. Power Application Systems*, vol. PAS-98, pp. 116-123, Jan./Feb. 1979.
- [4] J. A. Ferreira, *Electromagnetic Modeling of Power Electronic Converters*, Kluwer Academic Publishers: Boston-Dordrecht-London, 1989.
- [5] J. A. Ferreira, "Improved analytical modeling of conductive losses in magnetic components," *IEEE Trans. Power Electronics*, vol. 9, No. 1, pp. 127-131, Jan. 1994.
- [6] M. Bartoli, A. Reatti, and M. K. Kazimierczuk, "Modeling iron-powder inductors at high frequencies," *Proc. of 1994 IEEE-IAS Annual Meeting*, Denver, CO, Oct. 2-7, 1994, vol. 2, pp. 1225-1232.
- [7] M. Bartoli, A. Reatti, and M. K. Kazimierczuk, "Predicting the high-frequency ferrite-core inductor performance," *Proc. of Electrical Manufacturing & Coil Windings Association Meeting*, Rosemont, Chicago, IL, USA, Sept. 27-29, 1994, pp. 409-413.
- [8] M. Bartoli, A. Reatti, and M. K. Kazimierczuk, "High-frequency models of ferrite cores inductors," *Proc. of IECON'94*, Bologna, Italy, Sept. 5-9, 1994, pp. 1670-1675.